Available online at www.sciencedirect.com
SCIENCE DIRECT®
Polymer 44 (2003) 6335–6344
polymer
www.elsevier.com/locate/polymer

Adsorption of disulfide-modified polyacrylamides to gold and silver surfaces as cushions for polymer-supported lipid bilayers

J.C. Munro, C.W. Frank*

Department of Chemical Engineering, Stanford University, 381 North-South Mall, Stanford, CA 94305-5025, USA

Received 16 April 2003; received in revised form 30 June 2003; accepted 2 July 2003

Abstract

Inclusion of a polymer cushion between a lipid bilayer membrane and solid surface has been suggested as a means to provide a soft, deformable layer that will allow for transmembrane protein insertion and mobility. In this study, we evaluate the properties of a disulfide- and lipid-modified polyacrylamide polymer cushion. High molecular weight random copolymers with various degrees of disulfide and lipid substitution were synthesized. X-ray photoelectron spectroscopy (XPS) was used to determine quantitatively the percentage of disulfide groups bound to gold and silver surfaces. A quartz crystal microbalance with dissipation (QCM-D) was used to study the adsorption process and resulting film properties in situ. The presence of backbone–surface interactions leads to a competition between physisorption of the acrylamide backbone and chemisorption of the disulfide side-chains. This competition limits the degree of chemisorption to gold and silver surfaces. For a polyacrylamide with 10 mol% disulfide side-chains, 78% of the side-chains covalently bind to silver and only 41% bind to gold. The undesired physisorption of the acrylamide backbone leads to adsorption of the homopolymer itself. In addition, film thicknesses, as indicated by both XPS and QCM-D, are limited to 15–30 Å. The QCM-D results for all films indicate the formation of relatively rigid films, rather than the soft, deformable films desired for a lipid membrane polymer cushion.

Keywords: Lipopolymer; Polymer adsorption; Quartz crystal microbalance

1. Introduction

Supported lipid bilayer systems have been used to study the structure and function of biomembranes for several years [1]. Fundamental studies on cellular immune responses [2], membrane ligand–receptor interactions [3,4] membrane adhesion and fusion [5], and numerous other biophysical phenomena [6,7] have been conducted. In addition, several proposals have been made to use various bilayer systems for biosensors [8–10]. Supported bilayers formed on materials such as hydrophilic glass show good fluidity due to a thin (10–20 Å) lubricating layer of water [11–13]. However, lipid mobility is often suppressed on many other solid substrates such as metals and metal oxides [14,15]. In addition, large transmembrane proteins inserted into solid-supported bilayer systems often lose their lateral mobility due to interactions between the surface and protein domains that extend beyond the confines of the bilayer, making contact with the solid substrate [16–18].

In order to create a large enough separation between the lipid bilayer and solid substrate to allow protein mobility, many authors have suggested incorporating a soft, deformable hydrophilic polymer cushion between the lipid bilayer and solid substrate as described in a review by Sackmann [7]. Many designs have been proposed for polymer-supported lipid bilayer systems. Several authors have adsorbed polyelectrolytes such as polyethylenimine to charged substrates such as quartz and mica and subsequently performed Langmuir–Blodgett transfer or vesicle fusion to form a lipid bilayer [19–22]. Others have supported bilayers on thin films of polymers such as polyacrylamide [23], agarose [6], and dextran [24]. More complicated systems that provide covalent bonding of the polymer to the solid substrate as well as anchoring of the polymer support to the lipid bilayer have also been constructed. Several studies have focused on polymer systems on glass substrates where silanes act to covalently bond the polymers to the substrate [25–27]. Glass substrates

* Corresponding author. Tel.: +1-650-723-4573; fax: +1-650-723-9780.
E-mail address: curt.frank@stanford.edu (C.W. Frank).

0032-3861/$ - see front matter © 2003 Published by Elsevier Ltd.
doi:10.1016/S0032-3861(03)00659-1

also allow lipid mobility to be studied via fluorescence recovery after photobleaching. Wagner and Tamm used a telechelic poly(ethylene glycol) chain functionalized with a lipid on one end and a trimethoxysilane on the other [25]. Shen et al. [26] and Naumann et al. [27] used a benzophenone-silane molecule [28] to photochemically attach both random copolymers and end-functionalized polymers containing lipid-like alkyl moieties to surfaces. In all three of these studies, the amphiphilic polymer molecules were organized at the air–water interface and then transferred to substrates via Langmuir–Blodgett techniques. Several other authors have attempted to use self-assembly of disulfide-containing lipopolymers to gold surfaces [29–32]. Disulfides are known to form strong covalent bonds with gold surfaces in the form of thiolates [33]. After the self-assembly process, vesicle fusion has been used to form bilayers on top of the polymer films.

Langmuir–Blodgett transfer and self-assembly both have advantages. Langmuir films are organized with the hydrophilic polymer cushion in the subphase and the lipid or lipid-like side-chains at the air–water interface. These organized films can then be transferred and the organization maintained on the surface. In addition, free lipids can be mixed with the lipopolymer in the Langmuir films to control the anchoring density in the distal lipid layer. By controlling the area of the Langmuir film, the thickness of the polymer cushion can be controlled. Meanwhile, self-assembly has the advantage of simplicity. Unlike Langmuir–Blodgett transfer where planar substrates are used, films can be self-assembled on surfaces with different geometries including closed geometries such as channels. Unfortunately, the organization of the amphiphilic molecules after self-assembly is difficult to ascertain. Finally, since the motivation for using polymer cushions to support bilayers is to allow the incorporation of transmembrane proteins, mechanisms to test protein functionality are required. Examples of transmembrane proteins include ion channels and other proteins that are capable of changing the conductance of the membrane, which can be detected electrically. Unlike glass, metal substrates offer a useful way to transduce electrical signals, which could be useful in biosensor applications [9,10].

Two of the key features of polymer-supported tethered lipid bilayers are that the polymer cushion be hydrophilic and deformable and that the polymer be covalently attached to the substrate. In previous work on self-assembled lipopolymer films, surface plasmon resonance (SPR) and electrochemical techniques have been used to monitor the self-assembly and vesicle fusion processes and to test the quality of the finished bilayers [10,29,34]. However, little work has been done to quantify the amount of bonding of the lipopolymers to gold or to measure the viscoelastic properties of the polymer cushions. In this study, we synthesized lipopolymers based on the design of Zentel and co-workers [32,34–36]. The random copolymers consist of an acrylamide backbone with lipid side-chains and disulfide-containing side-chains. Previous studies on these polymer films have provided thickness and swelling data from SPR experiments [32,34–36]. Also, grazing incidence Fourier transform infrared spectroscopy has been used to show that the self-assembly process does not induce any orientation of the lipid side-chains [35]. Finally, Hausch et al. provide evidence of chemisorption via the disulfide chains by attempting to desorb material with 2-mercaptoethanesulfonic acid [32]. This small molecule is able to displace physisorbed poly(*N*-isopropylacrylamide), but not disulfide-containing poly(*N*-isopropylacrylamide).

In this study, quantitative data on the adsorption of the lipopolymers on both gold and silver surfaces was obtained. X-ray photoelectron spectroscopy (XPS) provided quantitative evidence of chemisorption of lipopolymers via thiolate bonds to gold and silver surfaces. A quartz crystal microbalance with dissipation (QCM-D) was used to study the adsorption of the lipopolymers from aqueous solutions and to evaluate the viscoelastic properties of the self-assembled films in situ. The effects of disulfide modification as well as the nature of the metallic surface on film properties are discussed. Quantitative analysis of polymer cushion properties may help to identify the systems that have the appropriate viscoelastic properties to allow protein insertion.

2. Materials and methods

2.1. Synthesis

The lipopolymer used was based on a random copolymer developed by Zentel and co-workers [32,34–36]. In their reported synthesis, random copolymers were made from the hydrophilic monomers *N*-isopropylacrylamide or *N*,*N*-dimethylacrylamide and the reactive ester *N*-acryloxysuccinimide [32]. Subsequently, the succinimide side-groups were reacted with various amines, including 2-aminoethyl methyl disulfide for chemisorption to gold, 1,2-dimyristoyl-*sn*-glycero-3-phosphoethanolamine (DMPE) as the lipid side-chain, and an excess of either isopropylamine or dimethylamine. In their later publications, various amines were reacted with a *N*-acryloxysuccinimide homopolymer [34,36]. In those studies, 2-aminoethyl methyl disulfide and DMPE were still used, but the hydrophilic backbone consisted of acrylamide monomers formed by reacting the excess *N*-acryloxysuccinimide monomers with ammonia instead of isopropylamine. In addition, positively charged (2-aminoethyl)-trimethylammonium chloride and the neutral 1-amino-2(dimethylamino)-ethane were added to the polymer chain to control the charge. The details of this modified synthesis were not reported. The authors reported greater polymer swelling under humid air for the acrylamide backbone vs. the *N*,*N*-dimethylacrylamide backbone, due to the greater hydrophilicity of acrylamide vs. *N*,*N*-dimethylacrylamide [34,36].

Based on the reported swelling of the lipopolymers, we chose to synthesize a polymer with an acrylamide backbone [34,36]. We used the same disulfide and lipid groups. However, for the sake of simplicity we chose to eliminate the variable of charge control and thus did not incorporate (2-aminoethyl)-trimethylammonium chloride and 1-amino-2(dimethylamino)-ethane. The synthetic steps used to create our lipopolymer were taken from various literature sources, as described below. 2-Aminoethyl methyl disulfide was prepared following a procedure by Conner et al. [37]. The monomer, *N*-acryloyloxysuccinimide, and polymer, poly(*N*-acryloyloxysuccinimide) (pNAS), were prepared following a procedure by Mammen et al. [38]. Next, DMPE and 2-aminoethyl methyl disulfide were reacted with pNAS as described by Hausch et al. [32]. Finally, aminolysis of the remaining active ester groups was performed following a procedure by Mammen et al. [38]. Purification of the polymers was conducted by diafiltration of the reaction mixture against water (Millipore, 18.2 MΩ) using a stirred cell (Amicon model 8010, Millipore Corp., Bedford, MA) equipped with a regenerated cellulose 5,000 M_w cutoff membrane (PLCC 25 mm, Millipore Corp, Bedford, MA). Following extensive diafiltration of the reaction mixture, we freeze-dried the materials. Materials were stored dry, under N_2 at −20 °C. Materials were characterized by NMR and FTIR (data not shown). The molecular weight of the materials was determined from the intrinsic viscosity of a polyacrylamide sample based on viscometry measurements using an Ubbelohde viscometer and Mark–Houwink parameters from the literature [39].

2.2. X-ray photoelectron spectroscopy

XPS was conducted on a Surface Science Instruments (SSI, Mountain View, CA) S-probe surface spectrometer using a monochromatic Al Kα X-ray source ($h\nu = 1486.6$ eV). Spectra were acquired at a detection angle of 35°, where the detection angle was defined as the angle between the surface and the axis of the analyzer lens. Binding energies were referenced to the Au $4f_{7/2}$ binding energy at 84.0 eV or to the Ag $3d_{5/2}$ binding energy at 368.3 eV. Substrates consisted of silicon wafers coated (in an Edwards Auto 306 evaporator, BOC Edwards, West Sussex, UK) with approximately 3 nm chromium and 100 nm of either gold or silver (Plasmaterials, Livermore, CA). After removal from the evaporator, substrates were placed directly in 1 mg/ml aqueous polymer solutions. Adsorption times varied from 30 min up to 72 h. Following adsorption, the samples were removed from the polymer solutions, rinsed with water, and dried under a stream of N_2. Samples were placed in the XPS chamber within 30 min of removal from solution. As performed by Hausch et al. to test for desorption, the polymer-coated samples were placed in 1 mM aqueous solutions of 2-mercaptoethanesulfonic acid (Aldrich, 98% purity, used as received) for 30 min, rinsed with water, and dried under a stream of N_2 [32]. For bound thiol controls, self-assembled monolayers of 1-hexadecanethiol (Fluka, 95% purity, used as received) were formed on gold and on silver. To do so, substrates were placed in 1 mM ethanolic solutions of 1-hexadecanethiol for 3 h, rinsed with ethanol, and dried under a stream of N_2.

2.3. Quartz crystal microbalance with dissipation

QCM-D was conducted on a Q-Sense D300 (Q-Sense AB, Gothenburg, Sweden) fitted with a QAFC 301 axial flow chamber. The QCM-D technique is described elsewhere [40]. In summary, a quartz crystal is driven at its resonance frequency of 5 MHz or at one of its first three overtones, 15, 25, or 35 MHz. Then the drive circuit is short-circuited and the exponential decay of the oscillation amplitude is monitored. The dissipation is obtained from the exponential decay constant that describes the decaying oscillation amplitude. AT-cut quartz crystals 14 mm in diameter and coated with a few nm titanium as an adhesion layer and about 100 nm of gold were purchased from Q-Sense, Inc. For measurements on gold, the quartz crystals were cleaned with oxygen plasma (75 W) for 2 min (March Plasmod Plasma Etcher, March Instruments, Inc., Concord, CA), soaked in ethanol (200 proof) for 10 min, and dried under a stream of N_2, as suggested by Ron et al. [41]. For measurements on silver, the front-side electrode of the gold-coated quartz crystal was coated with approximately 50 nm of silver in an Edwards Auto 306 evaporator. For reuse, silver-coated crystals were dipped in concentrated nitric acid for about 5 s to remove the silver, rinsed thoroughly with water, and then recoated with fresh silver. All measurements were conducted at 25.0 ± 0.03 °C. Frequency and dissipation changes (Δf and ΔD) were obtained at three harmonics (15, 25, and 35 MHz), with Milli-Q water used for the baseline. Polymer solutions at a concentration of 1 mg/ml were prepared using Milli-Q water. All polymers were soluble with minimal stirring. After equilibrating the QCM-D chamber in water, we rinsed approximately 0.5 ml of polymer solution through the measurement chamber, which has a volume of approximately 0.1 ml, over approximately 15 s. After a 30 min adsorption period, the chamber was rinsed with about 0.5 ml water over about 15 s.

3. Results

3.1. Synthesis

Following the above procedure, several polymers with varying degrees of DMPE and disulfide substitution were synthesized. The three polymers used in this study had the following stoichiometries as confirmed by NMR: PA—100 mol% acrylamide; $PA_{0.9}D_{0.1}$—90 mol% acrylamide, 10 mol% disulfide; and $PA_{0.9}D_{0.05}L_{0.05}$—90 mol% acrylamide, 5 mol% disulfide, 5 mol% DMPE. From viscometry,

the molecular weight of PA was approximately 2.1×10^6 g/mol, equivalent to a degree of polymerization of 30,400. This degree of polymerization is about 10 times greater than that reported for other pNAS polymers synthesized using the same procedure [38,42]. It is also about 125 times larger than the degree of polymerization reported by Hausch et al. for similar lipopolymers [32]. However, the reaction yield for the pNAS reaction was extremely low, around 5% compared to 98% as reported in the literature [38,42].

3.2. X-ray photoelectron spectroscopy

XPS was used to determine the dry thickness of the polymer films and to determine the chemical state of the disulfide species. As mentioned above, Hausch et al. argue that the lipopolymers are chemisorbed to gold via the disulfide side-chains rather than physisorbed via polymer backbone interactions with the surface based on the results of a competitive adsorption experiment monitored by SPR [32]. In that experiment, poly(*N*-isopropylacrylamide) and a copolymer containing 95 mol% *N*-isopropylacrylamide and 5 mol% of the 2-aminoethyl methyl disulfide side-chain were each adsorbed to a gold surface. Then the polymer coated substrates were placed in a 1 mM 2-mercapto-ethanesulfonic acid solution while being monitored by SPR. In the case of poly(*N*-isopropylacrylamide), SPR showed a decrease in film thickness from 19 to 6 Å, which was interpreted as displacement of the physisorbed polymer from the surface. Meanwhile, no thickness change was observed for the disulfide-containing polymer, which was taken as evidence that the polymer could not be displaced and was thus chemisorbed. Similar results were observed here. After exposure to a 1 mM 2-mercaptoethanesulfonic acid solution, the nitrogen peak in the XPS spectrum of the PA coated surface disappeared and a sulfur peak appeared (data not shown), indicating complete displacement of PA from the surface. Meanwhile, no changes in the XPS spectrum of $PA_{0.9}D_{0.1}$ coated surface were observed, indicating no displacement from the surface. To provide more direct evidence of chemisorption, we used XPS to quantify the amount of bound vs. unbound thiolate species.

3.2.1. Bound vs. unbound thiolate

Several authors have shown that sulfur atoms bound to gold or silver surfaces as thiolate species exhibit a sulfur $2p_{3/2}$ peak at 161.9 eV and $2p_{1/2}$ peak at 163.1 eV [43–45]. Unbound sulfur species show $2p_{3/2}$ binding energies at about 163.9 eV and $2p_{1/2}$ binding energies near 165.1 eV. The sulfur 2p doublet peak has an area ratio of 2:1 between the $2p_{3/2}$ and $2p_{1/2}$ peaks. Fig. 1 shows high-resolution spectra of the sulfur 2p region for disulfide-containing polymers adsorbed on gold for 72 h (Fig. 1(a)) and on silver for 20 h (Fig. 1(b)) and for a 1-hexadecanethiol SAM on silver (Fig. 1(c)). Four Gaussian peaks, representing the bound and unbound thiolate 2p doublets, were fit to the data.

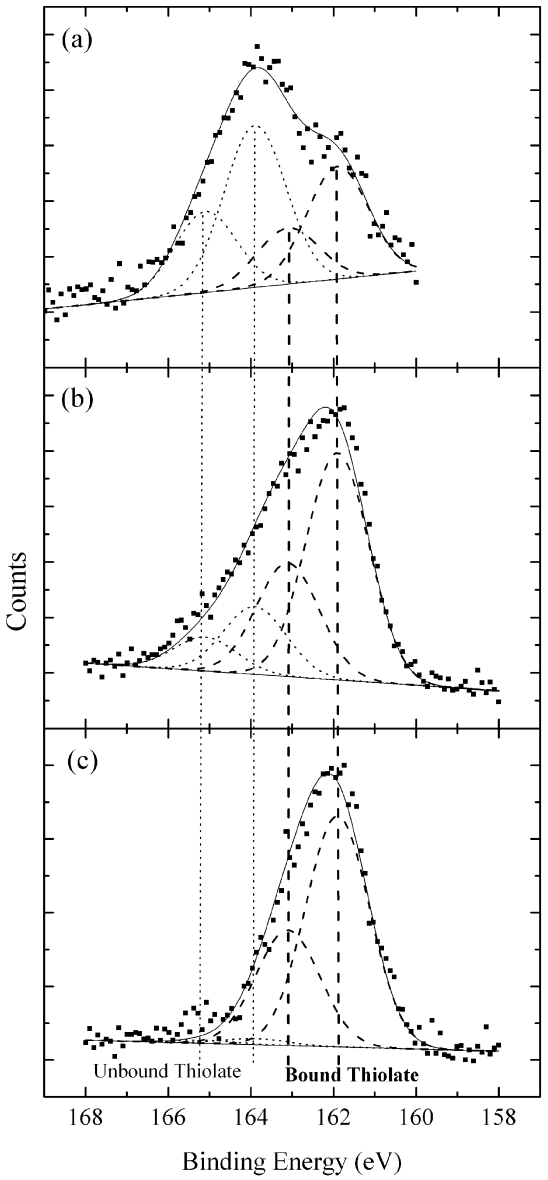

Fig. 1. High-resolution S(2p) XPS peaks and peak fits for (a) $PA_{0.9}D_{0.1}$ on Au; (b) $PA_{0.9}D_{0.1}$ on Ag; (c) 1-hexadecanethiol on Ag. (■) XPS Data; (· · · ·) unbound thiolate peak fits at 163.9 and 165.1 eV; (- - -) bound thiolate peak fits at 161.9 and 163.1 eV; and (—) sum of four peak fits.

The peak positions and 2:1 area ratio (as described above) for each doublet were fixed. In order to increase the signal-to-noise ratio, 100 scans were collected for each sample, reducing the standard error of the baseline to about 1%. The percentage of bound sulfur atoms was determined from the ratio of the areas of the two peaks representing the bound thiolate species (161.9 and 163.1 eV) to the total area of all four peaks. For $PA_{0.9}D_{0.1}$, 41 ± 11% of sulfur atoms are bound on gold, compared to 78 ± 7% on silver, where the standard errors represent the statistical accuracy of the measurement of the relative areas of the two sulfur 2p doublets. Meanwhile, as expected, nearly all (99%) sulfur atoms are bound for the SAM on silver. Note that the sulfur-containing moiety on the polymer is a disulfide. When a

disulfide binds to a surface, the sulfur–sulfur bond is cleaved and two separate thiolates result [33]. Therefore, in this system only half of the bound sulfur atoms tether the polymer to the substrate. However, the percentage of bound side-chains is still equivalent to the percentage of bound thiolate species.

3.2.2. Film thickness

XPS was also used to obtain dry film thickness values. Thicknesses were obtained from the attenuation of the gold or silver signal. For a clean substrate, the atomic percent of gold or silver would be 100%. The thickness, t, was found using the formula

$$\mathrm{At\%}_{\mathrm{Au\ or\ Ag}} = \exp[-t/(\lambda \cos\theta)] \quad (1)$$

where $\mathrm{At\%}_{\mathrm{Au\ or\ Ag}}$ is the atomic percent of gold or silver in the sample determined from the elemental analysis, λ is the inelastic mean free path of electrons through the overlayer, and θ is the detection angle. λ was estimated to be 28 Å by matching the thickness of the SAMs to values reported in the literature [46,47]. Film thicknesses for a 30 min adsorption time are reported in Table 1.

3.3. Quartz crystal microbalance with dissipation

3.3.1. Adsorption profiles

Adsorption profiles for PA, $PA_{0.9}D_{0.1}$, and $PA_{0.9}D_{0.05}L_{0.05}$ on gold and silver surfaces are shown in Fig. 2. Each polymer solution was tested several times. These are representative data sets. Δf and ΔD are shown at 15 MHz with water as the baseline. The dips at 0 and 30 min in the adsorption profiles are due to the mechanical disturbance to the crystal when liquid is flowing through the chamber. Flow occurs as an impinging jet on the center of the crystal with liquid flowing out around the edge of the crystal. The small Δf and ΔD changes near 27 min are due to a temperature change in the chamber. The chamber is maintained at 25.0 °C, but when liquid at room temperature (~20 °C) is exchanged in the small warm-up loop in the QCM-D chamber, the load on the heating element changes, causing a small temperature change. In general, it takes 3–4 min for Δf and ΔD to recover.

Table 1
XPS dry film thickness and QCM-D in situ film thickness values

Film/surface	Thickness (Å)	
	XPS	Sauerbrey film
SAM/Au	22	–
SAM/Ag	24	–
PA/Au	17	20
PA/Ag	19	28
$PA_{0.9}D_{0.1}$/Au	23	16
$PA_{0.9}D_{0.1}$/Ag	24	23
$PA_{0.9}D_{0.05}L_{0.05}$/Au	14	13
$PA_{0.9}D_{0.05}L_{0.05}$/Ag	19	14

3.3.2. Theory

The classical Sauerbrey equation (as shown below) states that the thickness of an adsorbed film is directly proportional to Δf :

$$\Delta f_n = -n\left(\frac{2\rho_f f_n^2}{\rho_q \nu_q}\right) t_f \quad (2)$$

where t_f is the film thickness, f_n is the resonance frequency of the crystal with no film at the nth harmonic, $\rho_q = 2650$ kg/m^3 is the density of the quartz, ρ_f is the density of the film, $\nu_q = 3340$ m/s is the shear velocity in quartz, and n is the harmonic number, which is the number of half-wavelengths of the thickness-shear waves in the crystal [48]. The Sauerbrey equation assumes the adsorbed film is of uniform thickness, is rigid, and obeys no-slip conditions at the interface between the crystal and film. These assumptions correspond to a loss-less film where $\Delta D = 0$.

Kanazawa and Gordon showed that for Newtonian liquids the following relationship holds:

$$\Delta f = n^{1/2} f_1^{3/2} (\eta_L \rho_L / \pi \mu_q \rho_q)^{1/2} \quad (3)$$

where f_1 is the fundamental frequency of the crystal in air, η_L and ρ_L are the viscosity and density of the liquid, and $\mu_q = 2.947 \times 10^{10}$ kg m^{-1} s^{-2} is the shear modulus of quartz [49]. Similarly, ΔD for Newtonian liquids is [50,51]:

$$\Delta D = 2(f_1/n)^{1/2} (\eta_L \rho_L / \pi \mu_q \rho_q)^{1/2} \quad (4)$$

In non-Newtonian liquids significant deviations from the Newtonian liquid equations can occur. Similarly, when an adsorbed viscoelastic film is present, the Sauerbrey equation may no longer apply. In both cases, Δf and ΔD become complex functions of the liquid and film properties.

3.3.3. Quantitative analysis

To begin the analysis of the QCM-D data, we determined how the Δf values scaled with the harmonic number. As seen in Eqs. (2) and (3), Δf scales linearly with the harmonic number for a solid film but as the square root of the harmonic number for a liquid. For all polymers and surfaces in this study, Δf scaled linearly with the harmonic number, consistent with the solid film prediction. For example, as shown for PA on silver in Fig. 3(b), Δf (15 MHz)/3, Δf (25 MHz)/5, and Δf (35 MHz)/7 all coincide with one another. Moreover, as shown in Fig. 2, the magnitudes of the ΔD values are quite small, no greater than about 0.8×10^{-6}. The linear scaling of Δf with the harmonic number and the small magnitudes of ΔD are both strong indications that thin, rigid films are formed.

3.3.4. Sauerbrey film

Using the Sauerbrey equation, film thicknesses were obtained from the Δf values. To remove any effects of the

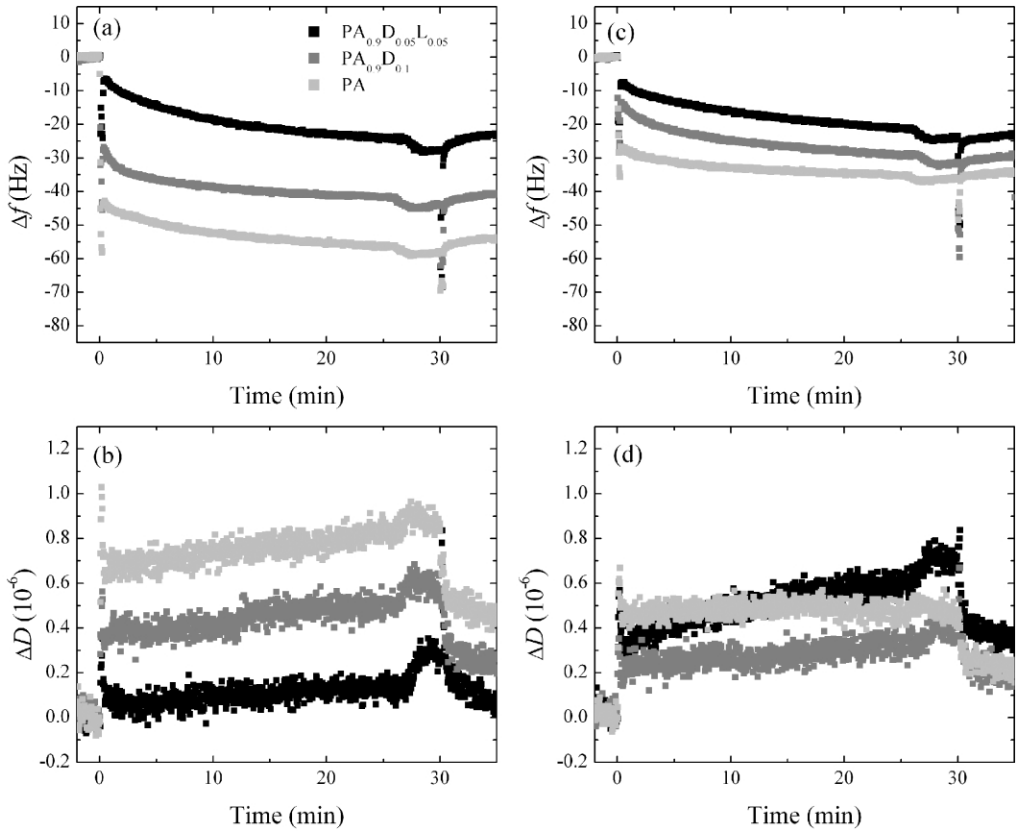

Fig. 2. QCM-D data at 15 MHz: (a) Δf for polymers on silver; (b) ΔD for polymers on silver; (c) Δf for polymers on gold; and (d) ΔD for polymers on gold.

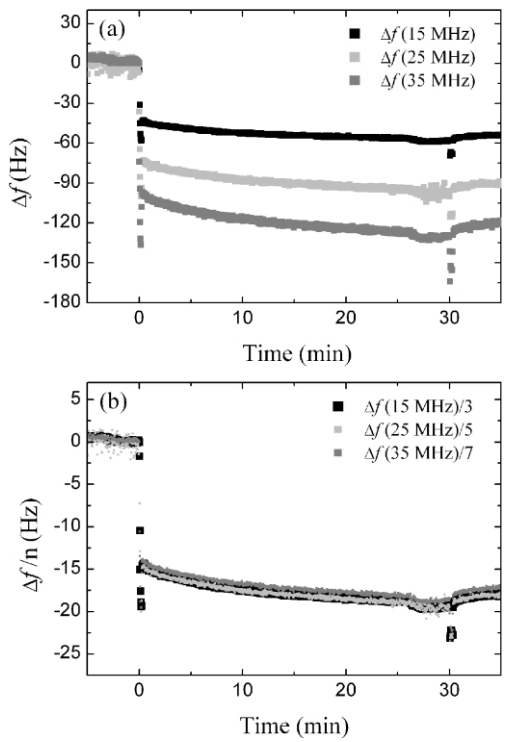

Fig. 3. QCM-D data for PA on silver at 15, 25 and 35 MHz: (a) unscaled Δf; and (b) Δf scaled by harmonic number, n.

bulk polymer solution, we used Δf values after the rinsing step at 35 min. That is, after the rinsing step we assumed there is an adsorbed polymer film on the surface surrounded by bulk water. As shown in Fig. 2, there are no significant differences in the Δf values before and after the water rinse, indicating no polymer film desorption took place. The two unknowns in the Sauerbrey equation (Eq. (2)) are the film density and film thickness. In order to calculate a thickness, we assumed a value for the film density, $\rho_f = 1100$ kg/m^3. This density value is comparable to the reported densities of polyacrylamide gels [52]. For each film, separate thickness values were obtained using Δf values at 15, 25, and 35 MHz (see Fig. 4). Then, these thickness values were averaged to obtain the final results, which are shown in Table 1.

Despite the simplicity of the Sauerbrey film model, the small magnitude of the ΔD values and the linear scaling of the Δf values indicate that a more complicated viscoelastic film model is not justified for these films. However, we have performed further experiments on unmodified polyacrylamides of molecular weights varying from 10^4 to 10^6 g/mol where viscoelastic film effects are apparent. An extensive analysis of those viscoelastic films is conducted in a separate publication [53].

3.3.5. Newtonian and non-Newtonian liquid effects

In addition to the frequency and dissipation responses caused by the formation of the thin, rigid polymer films, the

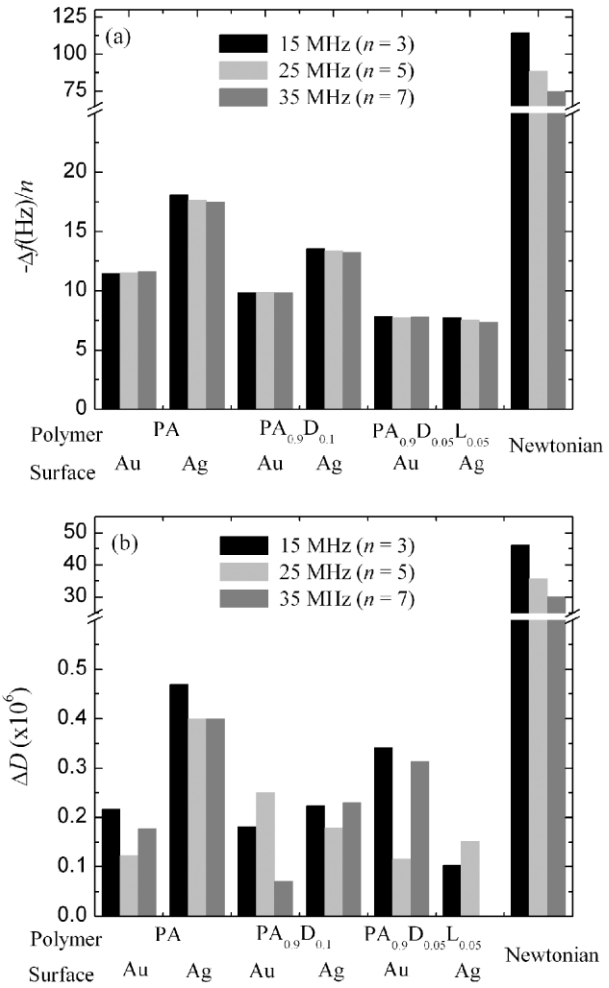

Fig. 4. Experimental and theoretical (a) Δf and (b) ΔD for all three polymers on gold and silver and for a Newtonian liquid with viscosity equal to that of the bulk polymer solutions, respectively.

effect of the bulk polymer solution on Δf and ΔD also needs to be considered. At 0 min in the adsorption runs, water was replaced by a bulk polymer solution. From viscometry, the 1 mg/ml PA solution has a viscosity of approximately 1.5×10^{-3} Pa s, compared to 8.9×10^{-4} Pa s for water at 25 °C. Viscosity values for $PA_{0.9}D_{0.1}$ and $PA_{0.9}D_{0.05}L_{0.05}$ were not measured, but are expected to be close to that of PA. If the polymer solutions were assumed to be Newtonian, Eqs. (3) and (4) could be used to calculate the theoretical Δf and ΔD values for changing from water to the viscous polymer solutions. The results of these calculations are shown in Fig. 4, where the following values were used: $f_1 = 4.95 \times 10^6$ Hz as obtained experimentally and $\rho_L = 1000$ kg m^{-3} for both water and the polymer solutions. These Δf and ΔD values are an order of magnitude greater than the experimental values that are also shown in Fig. 4.

In addition to the large changes in the Δf and ΔD values predicted for changing from water to the polymer solutions, similar changes would be expected upon exchanging the viscous polymer solutions for water. Such changes are not observed either. As seen in Fig. 2, at the rinsing step at 30 min, there were no significant changes in Δf and only small decreases in ΔD. Using a typical ΔD value of 0.2×10^{-6} at 15 MHz for the rinsing step, we can use Eq. (4) to predict the apparent viscosity difference between water and the polymer solutions. The predicted polymer solution viscosities are then 8.92×10^{-4} Pa s, just slightly higher than the 8.9×10^{-4} Pa s value for the viscosity of water. Next, Eq. (3) shows that Δf at 15 MHz for this small viscosity difference of 2.0×10^{-6} Pa s is only 1.3 Hz, which is close to the level of noise in the measurement.

The discrepancies between the experimental observations and the Newtonian liquid calculations can be explained by the non-Newtonian shear-thinning behavior commonly observed for aqueous polymer solutions [54,55]. Given the high operating frequency of the QCM-D, it is plausible that shear thinning of the bulk polymer solutions takes place, such that the polymer solution viscosity measured with the Ubbelohde viscometer is not an accurate representation of the viscosity sensed by the QCM-D.

This shear-thinning effect can be considered by comparing the characteristic relaxation time of the polymer to the characteristic time of the QCM-D, as done by Fu et al. [56]. The characteristic relaxation time of the polymer can be estimated by the Rouse time, τ_1 :

$$\tau_1 = 0.608 \frac{(\eta_0 - \eta_\infty) M_w}{cRT} \quad (5)$$

where c is the mass concentration of the polymer solution, R is the gas constant, and T is the temperature [54]. For example, for a 2.1×10^6 M_w, 1 mg/ml PA solution, $\tau_1 = 3.1 \times 10^{-4}$ s. Meanwhile, the characteristic time for the QCM-D—taken as the inverse of the operating frequency—at 15 MHz is 6.7×10^{-8} s and at 35 MHz is 2.9×10^{-8} s. Since τ_1 for the polymer solution is much longer than the characteristic time of the QCM-D, the instrument is unable to sense the viscous effects of the solution. Our results are also in excellent agreement with the theoretical treatment of non-Newtonian fluids by Nwankwo and Durning, who show that as τ_1 increases, both the inductance change and resistance change, which are related to Δf and ΔD, decrease and reach nearly zero for $\tau_1 = 10^{-5}$ [57]. We also discuss shear-thinning effects in a separate publication where the effects of polymer molecular weight and solution concentration are studied [53].

As a result of these non-Newtonian shear-thinning effects, the frequency and dissipation responses of the QCM-D measurements were dominated by film effects and not by bulk liquid effects.

4. Discussion

4.1. Physisorption vs. chemisorption

The only chemical moieties on these lipopolymers

designed to interact with the surface were the disulfide groups. However, as shown in Table 1, both XPS and the quantitative analysis of the QCM-D data indicate there is significant adsorption of the homopolymer PA to both gold and silver surfaces, comparable to the amount of adsorption of the disulfide-modified polymers. Homopolymer adsorption results from physisorption of the polymer backbone to the surface, which competes with chemisorption of the disulfide side-chains.

The balance between physisorption and chemisorption can be affected by several factors, including polymer chain mobility, concentration-dependent kinetic effects from adsorption, degree of substitution, and backbone–surface interactions. For example, Lenk et al. studied thiol-bound poly(methyl methacrylate) (PMMA) at room temperature [58]. PMMA is a rigid polymer with a characteristic ratio of about 10 [59]. For PMMA functionalized with 10 mol% thiol side-chains, the sulfur atoms were evenly distributed throughout the polymer layer, indicating that only a fraction of the thiols were bound to the surface. Meanwhile, Tsao et al. saw that almost all thiol species were bound to the substrate for a 5–10 mol% propanethiol-substituted poly (dimethylsiloxane), a highly flexible polymer with a characteristic ratio of about 6 [59,60]. Polyacrylamide, with a characteristic ratio of about 14, is similar to PMMA in its rigidity [59]. In addition, there may be significant backbone–surface interactions via van der Waals forces and via the nitrogen atoms in the acrylamide backbone units, which are able to form weak coordination bonds with gold and silver surfaces [61–63]. Similar to the results of Lenk et al. the XPS analysis shows that not all of the disulfide side-chains bind to the metal surfaces (78% of sulfur is bound to silver and 41% of sulfur is bound to gold). This indicates that the polymer mobility is limited, preventing all of the disulfide side-chains from finding the surface. However, note that these backbone–surface interactions are not strong enough to prevent the displacement of the PA homopolymer by 2-mercaptoethanesulfonic acid, which itself chemisorbs to the surface.

In addition, for each of the three polymers studied, both XPS and QCM-D indicate that slightly thicker films adsorb to silver than to gold surfaces. While thiols have similar affinity for gold and silver [64], weaker interactions occur between nitrogen and silver than between nitrogen and gold [63]. Stronger backbone–surface interactions on gold could cause the polymer chain to be spread out on the surface, allowing more backbone–surface contacts to form, and weaker interactions on silver could allow the polymer backbone to extend further from the surface, leading to thicker films.

4.2. Film structure

The QCM-D measurements show that all of the adsorbed films are rigid and thin, indicating that the chains adsorb in relatively flat conformations, with only short polymer loops and tails extending away from the surface. By comparing the observed thicknesses to the coil size of the free polymer in solution, we can estimate how flat the polymer conformation is on the surface. The radius of gyration (R_g) of the polymer coils can be estimated from the characteristic ratio of polyacrylamide, available in the literature [39]. For a 2.1×10^6 M_w polyacrylamide chain in water at 25 °C, $R_g \sim 1075$ Å, about 35 times larger than the film thicknesses measured. Given a repeat unit length of 2.52 Å for polyacrylamide, the experimental QCM-D thicknesses on silver correspond to 11 repeat units for PA, 9 repeat units for $PA_{0.9}D_{0.1}$, and 6 repeat units for $PA_{0.9}D_{0.05}L_{0.05}$. Again, this indicates that the chains lie quite flat on the surface with very short loops and tails.

4.3. XPS vs. QCM film thickness

Despite the dissimilar operating environments of the XPS and QCM-D, ultra-high vacuum vs. aqueous solution, there are only small differences in the measured film thicknesses for the two techniques. The thicknesses derived from the QCM-D indicate the formation of slightly thicker films for PA than for either of the disulfide-containing polymers. While PA may be able to swell slightly in situ, the bound thiols may prevent any similar swelling in the disulfide-modified polymers. As shown in Table 1, the dry film thicknesses measured by XPS for PA are slightly smaller than the in situ thicknesses. Meanwhile, the opposite is observed for the disulfide-modified polymers where the dry film thicknesses are comparable to or even slightly larger than the in situ values. Given that the λ and ρ_f parameters used in Eqs. (1) and (2) to calculate the XPS and QCM-D film thicknesses can only be estimated, these small discrepancies in the thickness values may not be significant.

4.4. Polymer cushion design

The strong physisorption of these acrylamides to gold and silver surfaces may prevent these lipopolymers from forming effective polymer cushions. Despite their hydrophilicity, QCM-D results indicate that the films are quite rigid. The 15–30 Å thicknesses are only slightly thicker than the water layer observed in solid-supported lipid bilayers. Therefore, these films may still not provide enough separation between the bilayer and solid substrate to allow transmembrane protein mobility. Considering the geometric design of this polymer system, it may be difficult to form a soft deformable layer that is well anchored in two parallel planes.

A polymer system with more control over the positions of the bilayer tethers and surface anchoring points would be beneficial. In a random copolymer like $PA_{0.9}D_{0.05}L_{0.05}$, there are a large number of lipid and disulfide moieties per chain. In addition, these moieties are separated, on average, by only 25 Å lengths of polymer backbone. Formation of multiple attachment points to the metal surface as well as

several tethering points to a bilayer above the polymer cushion creates a large number of constraints on the polymer chains. Once a few disulfide linkages are made to the surface, the polymer may quickly lose any mobility, hindering its ability to rearrange or deform. As shown in this study, it is difficult to control the number of groups that attach to the surface. A telechelic polymer system with only one surface anchoring group at one end of the chain and one lipid group on the other end of the chain would minimize the number of constraints on a single chain, allowing the hydrophilic backbone to adopt a more entropically favorable conformation and also allowing greater polymer mobility. Also, the surface density of attachment points for a telechelic system is equal to the number of adsorbed chains, which could be controlled with time of adsorption. In addition, the length of the hydrophilic polymer between the surface anchor and lipid can be controlled. The greater the distance between the bilayer tether and the surface anchor, the more mobile and deformable the chain can be. For the random polyacrylamide copolymer studied here, a thin, rigid layer is formed. In a study of another random copolymer system based on a poly(ethyloxazoline-*co*-ethylenimine) backbone, similar, small thicknesses of about 30 Å were observed [26]. Meanwhile, a telechelic system based on a polyethyloxazoline backbone had a thickness of about 80 Å [27].

5. Conclusions

This study complements previous work conducted by other authors on these acrylamide-based lipopolymers. QCM-D and XPS results agree with the previously reported SPR results in terms of film thickness. In addition, these XPS and QCM-D results provide quantitative evidence on the amount of chemisorption that takes place and on the viscoelastic nature of the polymer films, respectively. XPS shows that for a polymer with 10 mol% disulfide substitution only 41% of the disulfide side-chains bind to gold and 78% to silver. Strong physisorption of the acrylamide backbone, via nitrogen–metal coordination bonds, limits the mobility of the polymer on the surface, hindering the ability of the disulfide side-chains to find and bind to the surface. In addition, as shown by QCM-D, this strong physisorption causes unmodified polyacrylamide chains to adsorb to gold and silver surfaces as well. The QCM-D analysis shows that all of the films studied form very thin (15–30 Å), rigid layers with only short loops and tails extending away from the surface.

These random acrylamide copolymers have many of the key features desired of a polymer-support for lipid bilayers: (i) the backbone is highly hydrophilic, (ii) there is specific chemisorption of the polymer to gold and silver surfaces via the disulfide side-chains, and (iii) there are lipid side-chains that could anchor the polymer cushion to the bilayer. However, this study shows quantitatively that there is poor control over the amount of chemisorption. This study also shows that the lipopolymers fail to form soft, deformable films, which could be critical to protein insertion and mobility. We note that the lipopolymers synthesized in this study have significantly higher molecular weights than those studied previously by Hausch et al., which could affect the amount of chemisorption and the viscoelastic properties of the adsorbed films. In addition, changing concentrations could also affect the results, but this was not studied here. However, the techniques used here provide quantitative data that is required to assess the potential of any lipopolymer for use as a polymer-support for a lipid bilayer.

Acknowledgements

We would like to thank Kay Kanazawa for his comments and suggestions on the QCM-D analysis. Financial support for the project was provided by a NSF Graduate Research Fellowship (J.C.M.), the NSF XYZ-on-a-chip program under DMR-9980799, and the Center on Polymer Interfaces and Macromolecular Assemblies (CPIMA), which is sponsored by the NSF-MRSEC program under DMR-9808677.

References

[1] Tamm LK, McConnell HM. Biophys J 1985;47(1):105–13.
[2] McConnell HM, Watts TH, Weis RM, Brian AA. Biochim Biophys Acta 1986;864(1):95–106.
[3] Helm CA, Knoll W, Israelachvili JN. Proc Natl Acad Sci USA 1991; 88(18):8169–73.
[4] Heyse S, Vogel H, Sanger M, Sigrist H. Protein Sci 1995;4(12): 2532–44.
[5] Helm CA, Israelachvili JN, McGuiggan PM. Science 1989;246(4932): 919–22.
[6] Dietrich C, Tampe R. Biochim Biophys Acta 1995;1238(2):183–91.
[7] Sackmann E. Science 1996;271(5245):43–8.
[8] Uto M, Araki M, Taniguchi T, Hoshi S, Inoue S. Anal Sci 1994;10(6): 943–6.
[9] Cornell BA, Braach-Maksvytis VLB, King LG, Osman PDJ, Raguse B, Wieczorek L, Pace RJ. Nature 1997;387(6633):580–3.
[10] Raguse B, Braach-Maksvytis V, Cornell BA, King LG, Osman PDJ, Pace RJ, Wieczorek L. Langmuir 1998;14(3):648–59.
[11] Koenig BW, Krueger S, Orts WJ, Majkrzak CF, Berk NF, Silverton JV, Gawrisch K. Langmuir 1996;12(5):1343–50.
[12] Bayerl TM, Bloom M. Biophys J 1990;58(2):357–62.
[13] Johnson SJ, Bayerl TM, McDermott DC, Adam GW, Rennie AR, Thomas RK, Sackmann E. Biophys J 1991;59(2):289–94.
[14] Groves JT, Ulman N, Boxer SG. Science 1997;275(5300):651–3.
[15] Groves JT, Ulman N, Cremer PS, Boxer SG. Langmuir 1998;14(12): 3347–50.
[16] Poglitsch CL, Sumner MT, Thompson NL. Biochemistry 1991; 30(27):6662–71.
[17] Hinterdorfer P, Baber G, Tamm LK. J Biol Chem 1994;269(32): 20360–8.
[18] Salafsky J, Groves JT, Boxer SG. Biochemistry 1996;35(47): 14773–81.
[19] Majewski J, Wong JY, Park CK, Seitz M, Israelachvili JN, Smith GS. Biophys J 1998;75(5):2363–7.

[20] Wong JY, Majewski J, Seitz M, Park CK, Israelachvili JN, Smith GS. Biophys J 1999;77(3):1445–57.
[21] Wong JY, Park CK, Seitz M, Israelachvili J. Biophys J 1999;77(3): 1458–68.
[22] Luo GB, Liu TT, Zhao XS, Huang YY, Huang CH, Cao WX. Langmuir 2001;17(13):4074–80.
[23] Kuhner M, Tampe R, Sackmann E. Biophys J 1994;67(1):217–26.
[24] Elender G, Kuhner M, Sackmann E. Biosens Bioelectron 1996;11(6–7):565–77.
[25] Wagner ML, Tamm LK. Biophys J 2000;79(3):1400–14.
[26] Shen WW, Boxer SG, Knoll W, Frank CW. Biomacromolecules 2001; 2(1):70–9.
[27] Naumann CA, Prucker O, Lehmann T, Ruhe J, Knoll W, Frank CW. Biomacromolecules 2002;3(1):27–35.
[28] Prucker O, Naumann CA, Ruhe J, Knoll W, Frank CW. J Am Chem Soc 1999;121(38):8766–70.
[29] Spinke J, Yang J, Wolf H, Liley M, Ringsdorf H, Knoll W. Biophys J 1992;63(6):1667–71.
[30] Erdelen C, Haussling L, Naumann R, Ringsdorf H, Wolf H, Yang JL, Liley M, Spinke J, Knoll W. Langmuir 1994;10(4):1246–50.
[31] Marra KG, Kidani DDA, Chaikof EL. Langmuir 1997;13(21): 5697–701.
[32] Hausch M, Zentel R, Knoll W. Macromol Chem Phys 1999;200(1): 174–9.
[33] Ulman A. Chem Rev 1996;96(4):1533–54.
[34] Theato P, Zentel R. Langmuir 2000;16(4):1801–5.
[35] Hausch M, Beyer D, Knoll W, Zentel R. Langmuir 1998;14(25): 7213–6.
[36] Theato P, Zentel R. J Marcomol Sci, Pure Appl Chem 1999;A36(7–8):1001–15.
[37] Conner MD, Janout V, Kudelka I, Dedek P, Zhu JY, Regen SL. Langmuir 1993;9(9):2389–97.
[38] Mammen M, Dahmann G, Whitesides GM. J Med Chem 1995;38(21): 4179–90.
[39] Orwoll RA, Chong YS. Polyacrylamide. In: Mark JE, editor. Polymer data handbook. New York: Oxford University Press; 1999. p. 247–51.
[40] Rodahl M, Hook F, Krozer A, Brzezinski P, Kasemo B. Rev Sci Instrum 1995;66(7):3924–30.
[41] Ron H, Rubinstein I. Langmuir 1994;10(12):4566–73.
[42] Wang JQ, Chen X, Zhang W, Zacharek S, Chen YS, Wang PG. J Am Chem Soc 1999;121(36):8174–81.
[43] Lu HB, Campbell CT, Castner DG. Langmuir 2000;16(4):1711–8.
[44] Himmelhaus M, Gauss I, Buck M, Eisert F, Woll C, Grunze M. J Electron Spectrosc Relat Phenom 1998;92(1–3):139–49.
[45] Castner DG, Hinds K, Grainger DW. Langmuir 1996;12(21):5083–6.
[46] Bain CD, Troughton EB, Tao YT, Evall J, Whitesides GM, Nuzzo RG. J Am Chem Soc 1989;111(1):321–35.
[47] Walczak MM, Chung CK, Stole SM, Widrig CA, Porter MD. J Am Chem Soc 1991;113(7):2370–8.
[48] Sauerbrey G. Z Phys 1959;155:206–22.
[49] Kanazawa KK, Gordon JG. Anal Chem 1985;57(8):1770–1.
[50] Rodahl M, Kasemo B. Sens Actuators, A 1996;54(1–3):448–56.
[51] Stockbridge CD. In: Katz MJ, editor. Vacuum microbalance techniques. Effects of gas pressure on quartz-crystal microbalances, vol. 5. New York: Plenum Press; 1966. p. 147–78.
[52] Hirata Y, Kato Y, Andoh N, Fujiwara N, Ito R. J Chem Engng Jpn 1993;26(2):143–7.
[53] Munro JC, Frank CW. Submitted for publication.
[54] Vlassopoulos D, Schowalter WR. J Rheol 1994;38(5):1427–46.
[55] Lopez FV, Pauchard L, Rosen M, Rabaud M. J Non-Newtonian Fluid Mech 2002;103(2–3):123–39.
[56] Fu TZ, Stimming U, Durning CJ. Macromolecules 1993;26(13): 3271–81.
[57] Nwankwo E, Durning CJ. Rev Sci Instrum 1998;69(6):2375–84.
[58] Lenk TJ, Hallmark VM, Rabolt JF, Haussling L, Ringsdorf H. Macromolecules 1993;26(6):1230–7.
[59] Kurata M, Tsunashima Y. Viscosity-molecular weight relationships and unperturbed dimensions of linear chain molecules. In: Brandrup J, Immergut EH, editors. Polymer handbook. New York: Wiley; 1989. p. VII/1–VII/60.
[60] Tsao MW, Pfeifer KH, Rabolt JF, Castner DG, Haussling L, Ringsdorf H. Macromolecules 1997;30(19):5913–9.
[61] Bharathi S, Fishelson N, Lev O. Langmuir 1999;15(6):1929–37.
[62] Ooka AA, Kuhar KA, Cho NJ, Garrell RL. Biospectroscopy 1999; 5(1):9–17.
[63] Michota A, Kudelski A, Bukowska J. Surf Sci 2002;502–503:214–8.
[64] Buttry DA, Ward MD. Chem Rev 1992;92(6):1355–79.